Polarizing beam splitters constructed of form-birefringent multilayer gratings

Rong-Chung Tyan, Pang-Chen Sun and Yeshayahu Fainman

Department of Electrical and Computer Engineering, University of California at San Diego
La Jolla, CA 92093

ABSTRACT

We introduce a novel polarizing beam splitter that uses the anisotropic spectral reflectivity (ASR) characteristics of a high spatial frequency multilayer binary grating. By combining the form birefringence effect of a high spatial frequency grating with the resonant reflectivity of a periodic multilayer structure, the ASR characteristics for the two orthogonal linear polarizations are obtained. Such ASR effects allow us to design an optical element that is transparent for TM polarization but reflective for TE polarization. The properties of the polarizing beam splitter are investigated using rigorous coupled-wave analysis. The design results show that an ASR polarization beam splitter can provide a high polarization extinction ratio for optical waves from a wide range of incident angles and a broad optical spectral bandwidth. Such ASR polarizing beam splitters are uniquely suitable for image processing and optical interconnection applications.

Keywords : polarizing beam splitter, high spatial frequency binary grating, multilayer structure, form birefringence, diffractive optical element, optical components.

1. INTRODUCTION

Polarizing beam splitters (PBS) are essential components for numerous optical information processing applications such as free-space optical switching networks[1], read-write magneto-optic data storage systems[2], and polarization based imaging systems[3]. These applications require that the PBS providing high extinction ratios tolerate a wide angular bandwidth, a broad wavelength range of the incident waves, and compact size for efficient packaging. Conventional PBS employing either natural crystal birefringence (e.g., Wollaston prisms) or polarization selectivity of multilayer structures (e.g., PBS cubes) do not meet these requirements. The Wollaston prism requires a large thickness to generate enough walk-off distance between the two orthogonal polarizations due to intrinsically small birefringence of the naturally anisotropic materials. An alternative design of Wollaston prisms[4] reduces the thickness considerably by taking advantages of periodic multilayer slab structures that possess form birefringence which is several times larger than that of natural birefringent materials. However, the fabrication of such a multilayer slab structure is a tedious and long process. PBS cubes are easier to fabricate, but they provide good extinction ratios only in a narrow angular bandwidth for a limited wavelength range[5]. Other designs which utilize form birefringent high spatial frequency surface relief gratings[6] and single-layer-coated dielectric slab[7], have also been proposed to reduce the size of the components and to simplify the fabrication process, however, they also suffer from low extinction ratio, small operating angular bandwidth, and limited wavelength range.

In this manuscript, we introduce a new PBS device that uses the unique properties of anisotropic spectral reflectivity (ASR) characteristics of a high spatial frequency multilayer binary grating. The new ASR mechanism is based on combining the effect of form birefringence of a high spatial frequency grating (i.e., grating period is much less than the wavelength of the incident field) with the resonant reflectivity of a multilayer structure. In the next section we first describe intuitively the principle of the ASR behavior of the high spatial frequency multilayer grating using Effective Medium Theory (EMT)[8]. Then we use Rigorous Couple-Wave Analysis (RCWA)[9], tools for an optimum design[10] of the PBS, where the EMT results are used as an initial estimate. In sections 3 and 4 respectively, we use RCWA to design the ASR polarizing beam splitters and characterize them in terms of polarization extinction ratios for operation with waves of wide angular bandwidth and broad wavelength range. The results demonstrate extremely high extinction ratios (e.g., 1000000:1) when the PBS is operated at a specified wavelength and angle of incidence. Furthermore, good average extinction ratios (from 800:1 to 50:1) can be obtained when the PBS is operated for waves of 20^o angular bandwidth with wavelength ranging from 1300nm to 1500nm. The conclusions and future research directions are discussed in section 5.

2. ANISOTROPIC SPECTRAL REFLECTIVITY

Consider a multilayer structure formed on a substrate by depositing alternating layers of dielectric materials with high and low indices of refraction, n_h and n_l respectively. Such a structure exhibits high reflectivity in a wide spectral bandwidth, particularly when the thickness of each layer corresponds to a quarter-wave optical thickness for the center wavelength. The reflectivity of the quarter-wave structure can be increased by increasing the value of the ratio n_h/n_l and the number of layers in the stack. Larger values of n_h/n_l also increase the spectral bandwidth of high reflectance. For a multilayer structure made of isotropic dielectric materials, the reflectivity spectrums for the two orthogonal linear polarizations are identical and therefore, hardly separable. To separate the reflectivity spectrums for the two orthogonal linear polarizations, we need to substitute one or both (i.e., high and low refractive indices) materials with birefringent materials. Such a multilayer structure of anisotropic materials will possess reflectivity spectrum bands centered at different wavelengths for the two orthogonal polarizations, thereby, providing the desired separation of reflectivity spectrums. However, since natural materials possess very small birefringence, the separation of the reflection spectral bands corresponding to the two orthogonal polarizations will be very limited. With our approach the separation of the reflection spectral bands for the two orthogonal linear polarizations can be considerably increased due to the high anisotropy[11] that can be obtained with form birefringence.

Form birefringence effects[12] appear in high spatial frequency gratings formed by isotropic dielectric materials. Due to the geometric anisotropy of the grating structure, the two orthogonally polarized optical fields, one parallel to the grating grooves (designated as TE field) and the other perpendicular to the grating grooves (designated as TM field), encounter different effective dielectric constants and thus acquire a phase difference between them. This is similar to that obtained in natural anisotropic materials. The magnitude of form birefringence depends on the geometric composition of the grating structure (including the dielectric indices and the shape of the grating)[10] as well as the angle between the incident field and the grating vector. It is important to note that the value of form birefringence is a few times larger than the birefringence obtained with naturally birefringent materials. This makes the high spatial frequency grating an excellent candidate for separating the reflectivity spectrums for the two orthogonal polarizations.

Under the normal incidence, the effective indices for the TE and TM polarizations of a surface-relief high spatial frequency binary grating can be estimated from the 2nd order EMT[8]:

$$n_{TE}^{(2)} = \left\{ n_{TE}^{(0)2} + \frac{1}{3}\left(\frac{\Lambda}{\lambda}\right)^2 \pi^2 F^2 (1-F)^2 \left(n_{III}^2 - n_I^2\right)^2 \right\}^{1/2} \tag{1}$$

$$n_{TM}^{(2)} = \left\{ n_{TM}^{(0)2} + \frac{1}{3}\left(\frac{\Lambda}{\lambda}\right)^2 \pi^2 F^2 (1-F)^2 \left(\frac{1}{n_{III}^2} - \frac{1}{n_I^2}\right)^2 n_{TE}^{(0)2} n_{TM}^{(0)6} \right\}^{1/2} \tag{2}$$

where F is the duty cycle of the grating defined by $F=1-a/\Lambda$ with a being the width of air gap in the grating (see Fig.1), Λ is the grating period, λ is the wavelength of the incident wave, n_I and n_{III} are the indices of air and the grating material, respectively, and $n_{TE}^{(0)} = \left[F n_{III}^2 + (1-F) n_I^2\right]^{1/2}$ and $n_{TM}^{(0)} = \left\{ n_{III}^2 n_I^2 / \left[F n_I^2 + (1-F) n_{III}^2\right] \right\}^{1/2}$ are the effective indices of refraction for TE and TM waves provided by the zero order EMT.

Figure 1a shows an example of a high spatial frequency multilayer binary grating. We use SiO_2 and Si, with refractive indices of 1.45[13] and 3.51[14] respectively (for a wavelength of 1.3μm) as the two materials for the multilayer structures because of their fabrication compatibility and low absorption coefficients in the near infrared region (this results in a low insertion loss). For operation of the form birefringent grating in the zero diffraction order we set the grating period equal to 0.5 μm and the duty cycle F = 0.5. Using second order EMT (eqs.1 and 2) we obtain the following effective refractive indices for the two materials $n_{TE,Si}^{(2)}$ = 3.25, $n_{TE,SiO_2}^{(2)}$ = 1.26 and $n_{TM,Si}^{(2)}$ = 1.71, $n_{TM,SiO_2}^{(2)}$ = 1.18. The effective indices of both materials are larger for TE polarization than for TM polarization. This means that in the spectral domain, the reflection band for TE polarization will be centered at a longer wavelength as compared with that for TM polarization. This ASR characteristic is the essential property needed to realize the PBS.

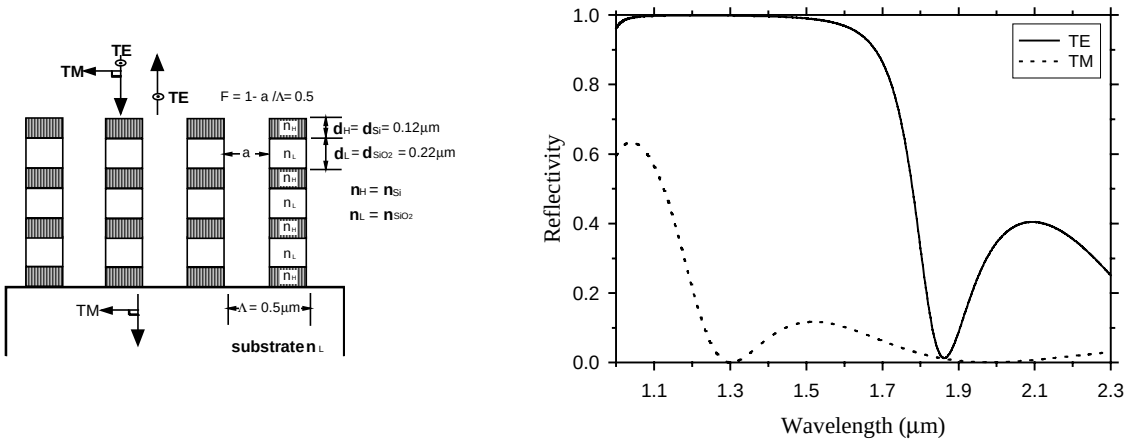

Fig. 1. (a) Schematic diagram of an ASR polarizing beam splitter operated with plane waves at normal incidence. (b) Numeric results of the reflectivity for TE and TM polarized waves vs. wavelength of a 7-layer PBS designed for normally incident waves.

Another characteristic is that the value of the effective index ratio for TE polarized light ($(n_h/n_l)_{TE}$=2.58) is larger than for TM polarized light ($(n_h/n_l)_{TM}$=1.45). This indicates that to achieve the same reflectance, the number of layers required by TE polarization will be less than that required by TM polarization. To minimize the number of layers needed to achieve a desired performance, we choose to maximize reflectivity for TE polarized light. Therefore, each layer has a quarter-wave optical thickness based upon the TE effective index. These values, estimated by EMT, are used as the basis for a more accurate design using RCWA. Optimization is done by incrementally varying the thickness of the layers to obtain the highest extinction ratio at the operational wavelength of 1.3 μm. To achieve broad reflectance peaks in the spectrum, we use high refractive index materials for both the first and the last layers in the structure. Figure 1b shows the numeric results of TE and TM reflectances as a function of the wavelength for a 7-layer high spatial frequency binary grating for normally incident optical fields. As expected, the reflectance peaks for TE and TM polarized light are separated and the TE polarization has a higher reflectance and broader bandwidth at longer wavelengths than the TM polarization. For the design wavelength of 1.3 μm, the TM polarized light will be transmitted while the TE polarized light will experience high reflectivity from the grating. The curves also show that the polarization extinction ratio remains high over a wide spectral range for the TM polarization. This feature allows the element to function as a low insertion loss polarizer. In fact, the sidelobe of the TM reflection is the only limit for the design of the polarization beam splitter. We anticipate that amplitude of the sidelobes may be reduced by fine-tuning other design parameters, such as the grating duty cycle. In the short wavelength region, both curves become irregular due to the coupling between the zero and the higher diffractive orders.

3. POLARIZING BEAM SPLITTER DESIGN

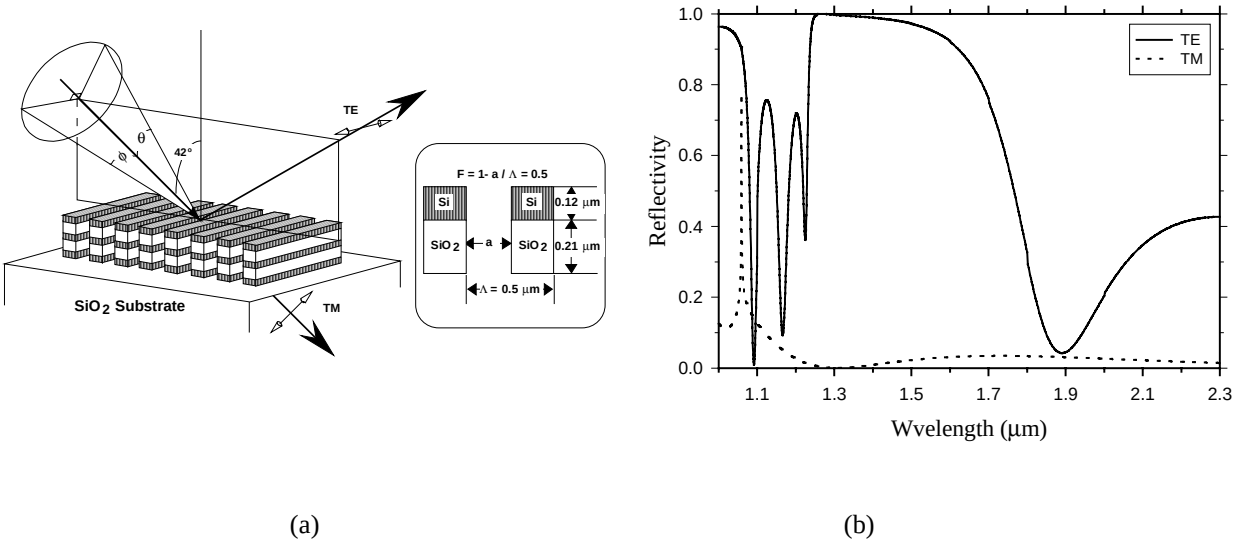

(a) (b)

Fig. 2. (a) Schematic diagram of a 5-layer ASR polarizing beam splitter operated with incident waves at an angle of 42^o. (b) Numeric results for the reflectivity of TE and TM polarized waves vs. wavelength for 42^o incidence.

To realize a useful PBS that will allow us to separate the path of the reflected wave (i.e., TE polarized wave in our design) from that of the incident wave, we investigate a PBS design that operates with waves at large angles of incidence. Consider a geometry shown in Fig. 2a, where the input wave vector is introduced at 42º angle of incidence, lying in the plane perpendicular to the grating grooves and parallel to the grating vector. This slanted incidence arrangement possess two additional advantages: 1) reflectivity from each layer for TE polarization is increased, thus only five layers were needed to achieve the desired performance (normal incidence required seven); 2) the sidelobe for the TM reflectivity is flattened, allowing operation of the beam splitter in a wider spectral range. Here again we used first the EMT estimates for an accurate RCWA design. The thickness of each layer was first chosen to be a quarter-wave of the wavelength for TE polarized wave, and then fine-turned to set the minimum of the TM reflectivity at the desired operating wavelength under the maximum band for the TE reflectivity. Since the reflection band for TE polarization is very wide, changing the thickness mostly affects the reflection band for TM polarization, and thus fine-tuning to achieve a desired performance is possible. Fig. 2b shows the numeric results of the reflectance vs. wavelength of the slanted incidence optical wave from the 5-layer grating. For the incident wavelength of 1.3μm, the TE and TM reflectances are 0.9971 and 0.0009128, and the polarization extinction ratio for reflection side of the beam splitter is better than 1100:1. The highest extinction ratio of 1000000:1 is obtained at the wavelength of λ= 1.265 μm. A relatively flat minimum zone of the TM reflectivity under the broadband of the TE reflectivity peak indicates that broadband operation is possible.

4. CHARACTERIZATION OF THE PBS PERFORMANCE

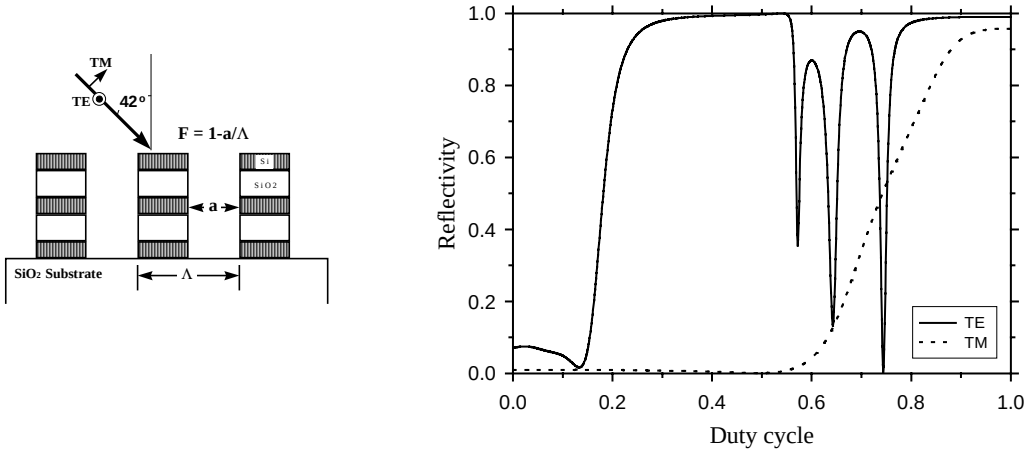

Fig. 3. Numeric results for the reflectivity of TE and TM polarized waves vs. duty cycle of the high spatial frequency binary grating. The design parameters are the same as using in Fig. 2a except the incident wavelength λ is now fixed at 1.3 μm and the duty cycle F is varying from 0 to 1.

In order to find the tolerance of the ASR polarizing beam splitter to possible fabrication errors, we numerically characterize the performance of the PBS by changing the duty cycle of the multilayer gratings. We use the same design parameters of the PBS shown in Fig. 2a, except that the incident wavelength λ is fixed at 1.3 μm and the duty cycle F is varied in the range 0 to 1.

The numeric results indicate that the reflectance of both polarizations stay approximately the same for the different duty cycles ranging from 0.3 to 0.55 (see Fig. 3). This shows high tolerance to fabrication errors of the ASR polarizing beam splitter. The reflectance of both polarizations become closer when the duty cycle approaches 0 and 1 and they become identical when the waves propagate at normal incidence.

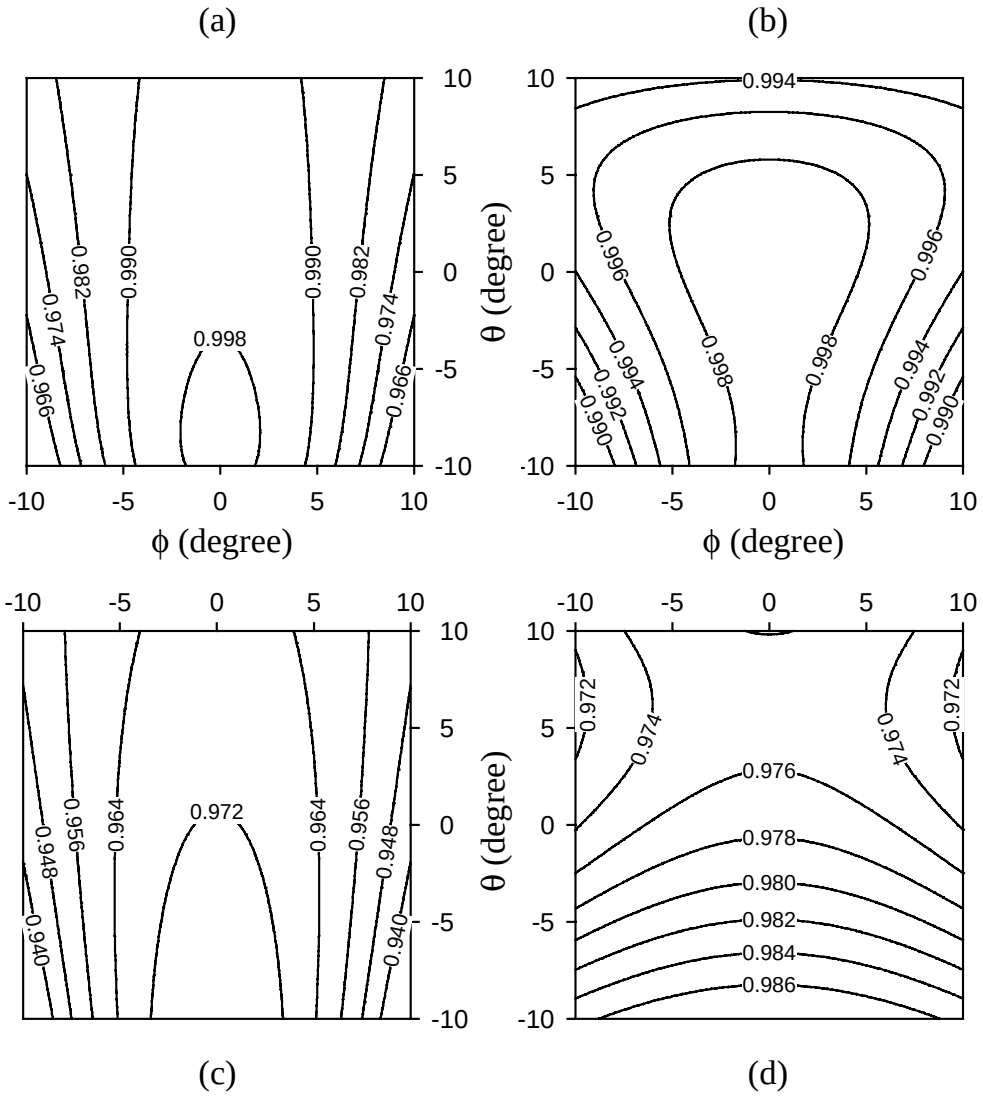

Fig. 4. Contour plots of TE reflectance and TM transmittance vs. incident angles (ϕ,θ) as defined in Fig. 2. (a) TE reflectance at wavelength λ=1.3 μm, (b) TM transmittance at wavelength λ=1.3 μm, (c) TE reflectance at wavelength λ=1.5 μm, and (d) TM transmittance at wavelength λ=1.5 μm .

We also investigate the angular dependence of the ASR polarizing beam splitter. As shown in Fig. 2a, the angles of incidence are varied to span an angular bandwidth of $\pm 10^{o}$ in both θ and ϕ directions defined around the initial 42^{o} bias angle. The results shown in Fig. 4 indicate that, at wavelength 1.3 μm, the reflectance for TE polarized light and the transmittance for TM polarized light are both better than 99% inside the 5^{o} angular bandwidth cone, and better than

97% inside the 10^o angular bandwidth cone. Around 1.5 μm results show that the TE reflectance and TM transmittance from this PBS are still better than 96% inside the 5^o angular bandwidth cone and better than 94% inside the 10^o angular bandwidth cone. These results indicate that wide angular bandwidth, as well as broad spectral range, of operation is possible using this design. The performance of the PBS can be further improved by adding more layers to increase the range of high TE reflectivity as well as bring the efficiency closer to 100%.

Fabrication of such PBS in the visible spectral range is a challenging task due to the need to fabricate a grating with sub-wavelength grating period. However, for near infrared range of operation, fabrication of the structure is practical. For example, in our design the total grating depth of 5 layers is only 0.78μm with the grating period 0.5μm, resulting in a grating aspect ratio of about 3:1, which is well within the fabrication capabilities of silicon microfabrication technology. Current thin film coating technology allows us to control the accuracy of the layer thickness within a few nanometers. Therefore, fabrication of the designed PBS (shown in Fig. 2a) can be done by first fabricating the multilayer structure, followed by direct e-beam lithography and ion beam etching a binary grating profile.

5. CONCLUSION

In conclusion, we have introduced a novel PBS device that is based on the ASR characteristics of a high spatial frequency multilayer binary grating. This PBS combines the form birefringence effect of a high spatial frequency grating with the high reflectance of multilayer structures. We use EMT for initial design and RCWA for optimization of the ASR polarizing beam splitter. We numerically characterize the ASR polarizing beam splitter in terms of polarization extinction ratio for operation with waves of wide angular bandwidth and broad wavelength range. The results show that the ASR polarizing beam splitter not only provides a very high extinction ratio for the two orthogonal polarizations, but also can be operated with optical signals of wide angular bandwidth and broad spectral range. From the numeric results, the fabrication error tolerance of the PBS has been shown to be very high. Another important advantage of the ASR polarizing beam splitters are their negligible insertion losses achieved by using non-absorbing dielectric materials. The ASR polarizing beam splitters combine such unique features as small size, negligible insertion losses, high polarization extinction ratios, and operation with waves of large angular bandwidth and broad spectral range. These features make these devices desirable for use in optical image processing, optical interconnections as well as other polarization optics applications.

6. ACKNOWLEDGMENTS

Authors thanks Paul Shames and Fang Xu for helpful discussions and preparation of the manuscript. This work was supported in part by the National Science Foundation, Advanced Research Projects Agency, Air Force Office Scientific Research and Rome Laboratory.

7. REFERENCES

1. F. B. McCormick, F. A. P. Tooley, T. J. Cloonan, J. L. Brubaker, A. L. Lentine, R. L.Morrison, S. J. Hinterlong, M. J. Herron, S. L. Walker, and J. M. Sasian, “Experimental

investigation of a free-space optical switching network by using symmetric self-electro-optic-effect devices," Appl. Opt. Vol.31, pp.5431-5446 (1992).

2. M. Ojima, A. Saito, T. Kaku, M. Ito, Y. Tsunoda, S. Takayama, and Y. Sugita, "Compact magnetooptical disk for coded data storage," Appl. Opt. Vol.25, pp.483-489 (1986).

3. P. Kunstmann and H.-J. Spitschan, "General complex amplitude addition in a polarization interferometer in the detection of pattern differences," Opt. Commun. Vol.4, pp.166-168 (1971).

4. K. Shiraishi, and S. Kawakami, "Spatial walk-off polarizer utilizing artificial anisotropic dielectrics, " Opt. Lett. Vol.15, pp.516-518 (1990).

5. J. L. Pezzaniti, and R. A. Chipman, "Angular dependence of polarizing beam-splitter cubes," Appl. Opt. Vol.33, pp.1916-1929 (1994).

6. M. C. Gupta and S. T. Peng, Proc. "Multifunction grating for signal detection of optical disk," *Optical Data Storage*, J. J. Burke, T. A. Shull, N. Imamura, ed.Vol.1499, pp.303-306, Proceedings of the SPIE - The International Society for Optical Engineering, (1991).

7. R. M. A. Azzam, "Polarizing beam splitters for infrared and millimeter waves using single-layer-coated dielectric slab or unbacked films," Appl. Opt. Vol.25, 4225 (1986).

8. S. M. Rytov, "Electromagnetic properties of a finely stratified medium,"Soviet Physics JETP, Vol.2, pp.466-475 (1956).

9. M. G. Moharam, and T. K. Gaylord, "Diffraction analysis of dielectric surface-relief gratings," J. Opt. Soc. AM. Vol.72, pp.1385-1392 (1982).

10. I. Ricther, P. C. Sun, F. Xu, and Y. Fainman, "Design considerations of form birefringent microstructures," Appl. Opt., Vol.34, pp.2421-2429 (1995).

11. F. Xu, R.-C. Tyan, P.-C. Sun, Y. Fainman, C.-C. Cheng, and A. Scherer, "Fabrication, Modeling and Characterization of Form Birefringent Nanostructures," Opt. Lett. (Accepted for publication in Dec. 1995).

12. M. Born, and E. Wolf, *Principles of Optics* , pp.705-708, Pergamon, Oxford, 1975.

13.H. R. Philipp, "Silicon dioxide (SiO_2) (glass)," *Handbook of Optical Constants of Solids*, E. D. Palik, ed., Vol.1, pp.749-763, Academic, Orlando, Fla.,1985

14.D. F. Edwards, "Silicon (Si)," *Handbook of Optical Constants of Solids*, E. D. Palik, ed., Vol.1, pp.547-569, Academic, Orlando, Fla.,1985

8. REFERENCES

[1] F. B. McCormick, F. A. P. Tooley, T. J. Cloonan, J. L. Brubaker, A. L. Lentine, R. L.Morrison, S. J. Hinterlong, M. J. Herron, S. L. Walker, and J. M. Sasian, Appl. Opt.**31**, 5431 (1992).

[2] M. Ojima, A. Saito, T. Kaku, M. Ito, Y. Tsunoda, S. Takayama, and Y. Sugita, Appl. Opt. **25**, 483 (1986).

[3] P. Kunstmann and H.-J. Spitschan, Opt. Commun. **4**, 166 (1971).

[4] K. Shiraishi, and S. Kawakami, Opt. Lett. **15**, 516 (1990).

[5] J. L. Pezzaniti, and R. A. Chipman, Appl. Opt. **33**, 1916 (1994).

[6] M. C. Gupta and S. T. Peng, Proc. Soc. Photo-Opt. Instrum. Eng. **1499**, 303 (1991).

[7] R. M. A. Azzam, Appl. Opt. **25**, 4225 (1986).

[8] S. M. Rytov, Soviet Physics JETP, **2**, 466 (1956).

[9] M. G. Moharam, and T. K. Gaylord, J. Opt. Soc. AM. **72**, 1385 (1982).

[10] I. Ricther, P. C. Sun, F. Xu, and Y. Fainman, Appl. Opt., **34**, 2421 (1995).

[11] F. Xu, R.-C. Tyan, P.-C. Sun, Y. Fainman, C.-C. Cheng, and A. Scherer, Opt. Lett. (Accepted for publication in Dec. 1995).

[12] M. Born, and E. Wolf, *Principles of Optics* (Pergamon, Oxford, 1975), pp. 705-708.

[13] E. D. Palik, ed.,*Handbook of Optical Constants of Solids* (Academic, Orlando, Fla.,1985), pp.547

[14] E. D. Palik, ed.,*Handbook of Optical Constants of Solids* (Academic, Orlando, Fla.,1985), pp.547